Linköping University Post Print

Optical properties and switching of a Rose Bengal derivative: A spectroscopic ellipsometry study

C Akerlind, Hans Arwin, Fredrik Jakobsson, H Kariis and Kenneth Järrendahl

N.B.: When citing this work, cite the original article.

Optical Properties and Switching of a Rose Bengal Derivative:

A Spectroscopic Ellipsometry Study

C. Åkerlind[1,2], H. Arwin[2], F. L. E. Jakobsson[3], H. Kariis[1], K. Järrendahl[2]

[1] Department of Information Systems, Swedish Defence Research Agency, SE 581 11

Linköping, Sweden,

[2] Department of Physics, Chemistry and Biology, Linköping University, SE 581 83

Linköping, Sweden,

[3] Department of Science and Technology, Linköping University, SE 601 74

Norrköping[*], Sweden

Contact corresponding author: **email**: christina.akerlind@foi.se, **phone:** +46 13 378525,

fax: +46 13 378519

Abstract

Optical properties in terms of the complex-valued dielectric function were determined for spin-coated films of a Rose Bengal derivative using variable angle of incidence spectroscopic ellipsometry in the visible and infrared wavelength regions. In addition, the thickness and roughness of the films were determined and related to the solution concentration of Rose Bengal. Switching between two different oxidation states of the Rose Bengal derivative was investigated. The two states were chemically induced by exposure to vapors of hydrochloric acid and ammonia, respectively. A substantial and reversible change of the optical properties of the films was observed.

---

[*] Fredrik Jakobsson, CDT Research, Cambridge Display Technology Limited
Greenwich House, Madingley Rise, Madingley Road, Cambridge, CB3 0TX, UK

1. Introduction

The possibility to change color of an object can be attractive in many disciplines and application fields. Materials with dynamic optical properties are explored for a wide range of applications, from printable organic electronics with electrochromic properties [1] to heat reflecting systems and camouflage applications [2].

Optical properties can be controlled in several ways, e.g. mechanically, electrically, thermally or chemically, giving possibilities to obtain a certain optical response in a specific wavelength region. One example is chemically induced color changes that some dye systems undergo due to acid or base exposure. In the work presented here, focus is on such effects in a Rose Bengal (RB) derivative. Rose Bengal has the structure [4,5,6,7-tetrachloro-2',4',5',7'-tetraiodo-fluorescein].

The RB molecule consists of a benzene and a xanthene moiety with substituents that determine the photophysical properties [3]. The derivative studied in this work has the substituent $R = NH(C_2H_5)_3$ attached to a negatively charged oxygen as well as to a carboxylic group to form a salt. This form is called the quinoid (q) form of RB and is shown to the left in Fig. 1. When exposed to vapor of hydrochloric acid (HCl), RB changes its conformation from its quinoid form to the lactone (l) form as shown to the right in Fig. 1 and when subsequently exposed to ammonia (NH_3) it changes back to the quinoid form. Chemically this corresponds to that the oxygen undergoes a

protonation/deprotonation reaction [3]. In this transformation it also changes its appearance from pink to transparent as the dominant absorption peak almost vanishes [3] and the electron delocalization over the xanthene is broken.
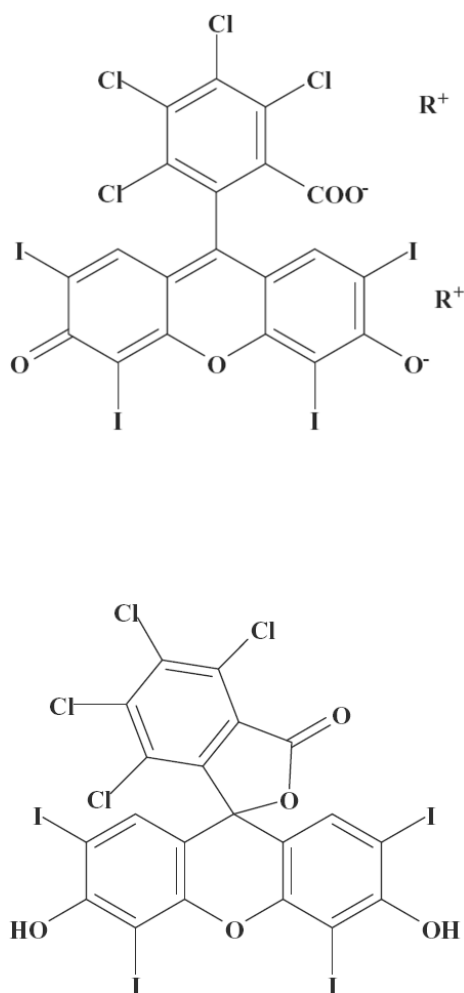
Figure 1. Molecular structure of Rose Bengal salt. The molecule consists of a benzene and a xanthene moiety which have substituents determining the photophysical properties. To the left is the quinoid (q) form and to the right is the lactone (l) form. In this study the substituent $R = NH(C_2H_5)_3$.

There are several other substances similar to RB, such as Fluorans, which is a common name for a type of leuco-dyes with the same basic molecular structure as RB in the lactone form [4]. These substances have a great variety of colors, depending on their different substituents.

RB has been used in organic electronics as an acceptor in photovoltaic devices [5]. Bi-stable organic memory devices utilizing the nonlinear conduction properties of RB have been reported, although the origin of the switching mechanism has been debated [6-9]. The control of layer thicknesses in these devices is crucial for the performance.

In this work we focus on determination of the optical properties and thicknesses of thin films of a RB derivative and study how chemically induced switching influences these properties. The studies are done using variable angle of incidence spectroscopic ellipsometry (VASE) [10] providing the full complex-valued optical response functions as well as structural information of the investigated samples. The information provided in this study will be of importance for research on organic electronic devices involving layers of RB.

2. Experimental details

Rose Bengal salt (from Sigma-Aldrich) was dissolved in 1-propanol to nominal concentrations of 8, 12, 16 or 20 mg/ml. The solutions were then filtered through a 0.1 µm filter. Thin films were formed by spin coating at 2000 rpm for 30 s on 1.5 x 1.5 cm^2 as received silicon substrates with native oxide as in the work by Jakobsson et al.[6]. All samples were prepared in a clean-room environment. A selection of the samples was later exposed to a saturated vapor of HCl or NH_3 for half a minute prior to subsequent measurements.

VASE was used to record the ellipsometric angles Ψ and Δ on thin films of RB in the spectral range from infrared (IR) to near ultraviolet or more specific from 0.038 to 5.03 eV (0.246 to 33.0 μm). Measurements on chemically unexposed films were done using a VASE-system (J.A. Woollam Co., Inc.) at photon energies in the range 0.73 to 5.03 eV (1698 - 246 nm) in steps of 0.05 eV at three angles of incidence (50°, 60°, 70°).

In the IR spectral region measurements were performed on a selection of unexposed samples with an infrared spectroscopic ellipsometer (IRSE, J.A. Woollam Co., Inc.) at photon energies in the range 0.038 - 0.62 eV (33 – 2 μm) with resolution $2.48 \cdot 10^{-4}$ eV (2 cm^{-1}) at three angles of incidence (50°, 60°, 70°).

The chemically exposed samples were necessary to measure within minutes after exposure. A real-time dual rotating compensator ellipsometer (RC2, J.A. Woollam Co., Inc.) was therefore used with the range 0.73 to 5.03 eV (1698 – 246 nm) at an incident angle of 70°.

Analysis of the ellipsometric data was made with the WVASE32 software (J.A. Woollam Co., Inc.) [10]. The optical properties in terms of the complex-valued dielectric function $\varepsilon = \varepsilon_1 + i\varepsilon_2$ were modelled by combining several dispersion models. Cauchy dispersion [11] with an Urbach absorption tail was used to describe the optical background whereas resonance peaks were described using Lorentz oscillators [12]. Three parameters were used to describe the peaks; the amplitude A, the energy En and the broadening Br. A total of four oscillators were used. Two of them are near-lying and

were modelled using a Gauss-Lorentz Asymmetric Doublet oscillator feature (GLAD) included in the WVASE software [10]. Values of all parameters are presented after rounding off to the number off significant digits defined by 90% confidence intervals in the fitting procedure.

The sample model consists of a number of isotropic and homogeneous layers representing the substrate, films and ambient. The model parameters of interest to determine were fitted using the Levenberg-Marquardt algorithm to match model data to experimental Ψ- and Δ-data using the mean square error (MSE) [13] as a measure of the goodness of fit. The sample model used was either a four-phase (substrate / overlayer / film / ambient) system or a five-phase (substrate / overlayer / film / roughness / ambient) system. The silicon substrate and overlayer were represented by well defined optical reference data for Si and SiO_2, respectively [14]. The roughness was described using a common approach [15] with a Bruggeman effective medium approximation (EMA) layer with 50% void and 50% of the underlying Rose Bengal film properties. All measurements were performed in an air ambient.

When several variables are varied there are multiple solutions and data correlation can be high. A multiple sample analysis (MSA) [16] was therefore used to reduce correlation problems and served as an initial starting point in the analysis. In the MSA, data recorded from several samples were fitted simultaneously assuming the same optical properties for the RB layer in all samples, but with each layer having different thicknesses.

The results from the MSA were then used as input values in the analysis of each sample. The output from the optical characterization were the optical properties $\varepsilon = \varepsilon_1 + i\varepsilon_2$ as well as the thickness and roughness of the RB films.

3. Results and Discussion

The thickness of the overlayer on the substrates was determined on a silicon sample form the same wafer as those used for the RB spin coating which was performed in a clean room atmosphere. The resulting thickness of 1.7 nm was used as a fixed value in the optical modeling.

Modeling using a four-phase system and MSA gave film thicknesses of the RB layer between 15.6 nm and 38.6 nm depending on the solution concentration as shown in Table 1. Separate analysis of the four samples gave similar thicknesses as also shown in Table 1 but the resulting optical properties of the RB layers showed differences motivating an improved model. Therefore, a five-phase model was applied with an added EMA-layer representing surface roughness. The four samples where analyzed separately giving film and roughness thicknesses according to Table 2. The thickness of the roughness layer and the RB layer add up to a total thickness in agreement with the previous analysis especially when considering the lower density of the roughness layer. The fraction of the roughness thickness compared to the total thickness (RB layer and roughness layer) decreases with concentration. The absolute value of the roughness is however similar for the three thickest RB layers. These results indicate that the RB films prepared with lower concentrations (8 mg/ml), besides being thinner, most probably also have a more dense structure which can not be resolved from the present

data. Possible mechanisms could be that the near-substrate part of the RB-layer, due to substrate interaction, is different in terms of density and may even show anisotropic effects. Furthermore, for this low concentration the possibility that the film is discontinuous can not be excluded and will be a topic in future studies. It should also be noted that RB is known to aggregate at high concentrations which can influence the formation of thicker films [17]. The thickness results can be compared with single wavelength ellipsometry and Atomic Force Microscopy (AFM) measurements on similarly prepared RB films giving thicknesses between 10 and 30 nm [6].

Table 1. Results from the four-phase system modeling

Concentration [mg/ml]	8	12	16	20
Thickness of RB layers (MSA) [nm]	15.6	23.7	25.7	38.6
Thickness of RB layers (separate analysis) [nm]	15.7	24.2	25.9	38.6

The five-phase model data fit the experimental data very well for both of the ellipsometric parameters Ψ and Δ and for all angles as seen in Fig. 2.

Table 2. Results from the five-phase system modeling

Concentration [mg/ml]	8	12	16	20
Thickness of RB layers [nm]	10.0	20.7	23.2	36.2
Thickness of roughness layer [nm]	6.5	3.9	3.2	3.6
Roughness / total thickness [%]	39	16	12	9
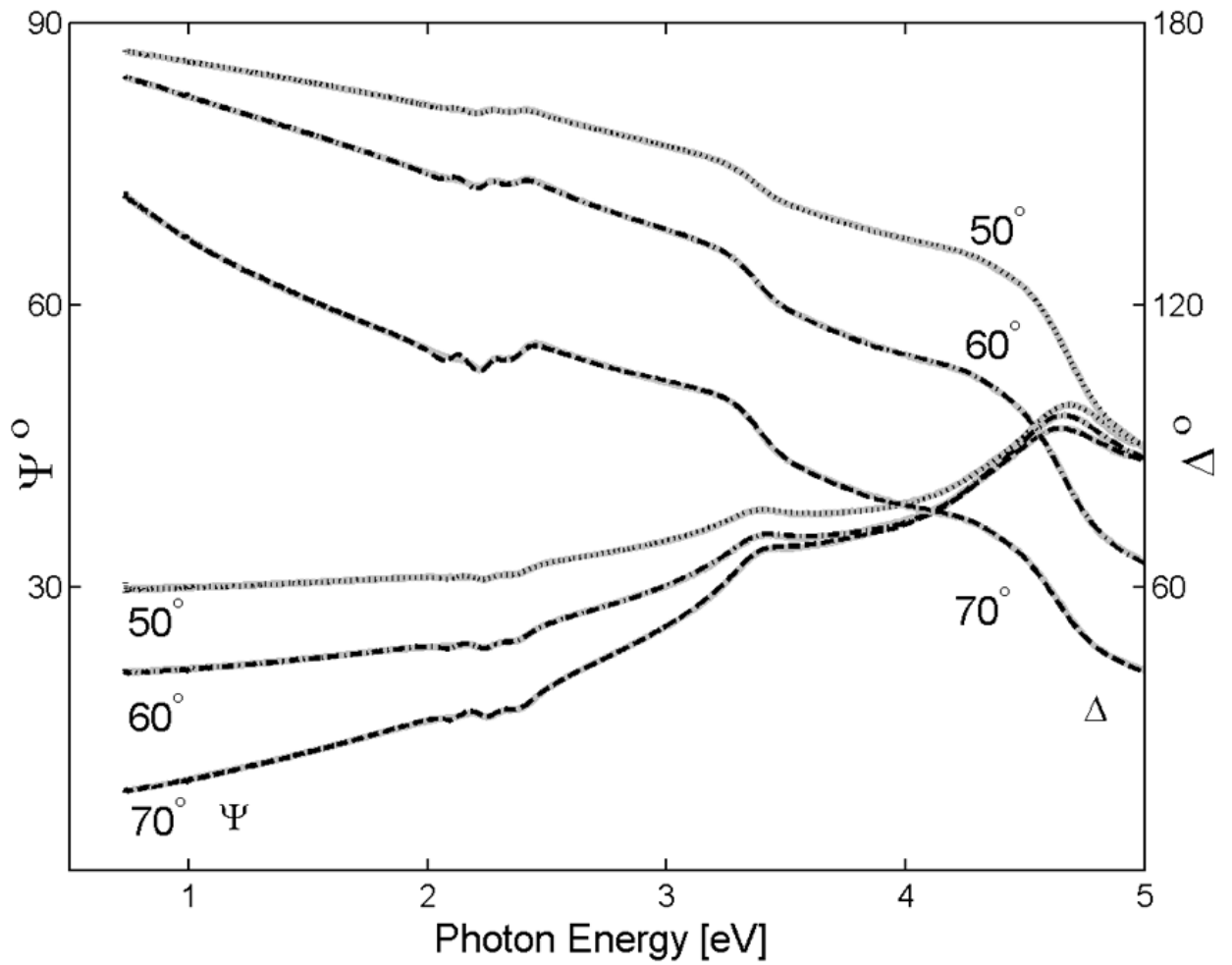
Figure 2. A representative model fit to experimental Ψ and Δ data for a RB sample prepared from a 12 mg/ml solution.

The resulting optical properties of RB layers in terms of $\varepsilon = \varepsilon_1 + i\varepsilon_2$ obtained using a five-phase model are shown in Fig. 3. The properties of the three thicker films are close to each other whereas the properties extracted from the sample with the thinnest RB film differ. This film also has higher roughness then the rest of the films. The location (En_i) and the broadening (Br_i) of the different absorption peaks for each of the samples can be found in Table 3.

Table 3. Results from the five-phase system modeling. For each of the four resonances (i = 1, 2, 3, 4) En_i is the position of the peak, A_i is the amplitude and Br_i is the broadening.

Conc. [mg/ml]	MSE	En_1 [eV]	A_1	Br_1 [eV]	En_2 [eV]	A_2	Br_2 [eV]	En_3 [eV]	A_3	Br_3 [eV]	En_4 [eV]	A_4	Br_4 [eV]
8	1.0	2.18	2.47	0.13	2.35	0.76	0.13	4.80	0.87	0.75	5.55	2.1	1.33
12	1.5	2.18	2.06	0.13	2.35	0.71	0.13	4.79	0.64	0.60	5.49	1.8	1.22
16	1.8	2.17	2.15	0.13	2.35	0.73	0.13	4.78	0.65	0.64	5.60	2.0	1.19
20	5.0	2.17	2.36	0.13	2.36	0.77	0.13	4.75	0.48	0.50	5.62	2.4	1.23
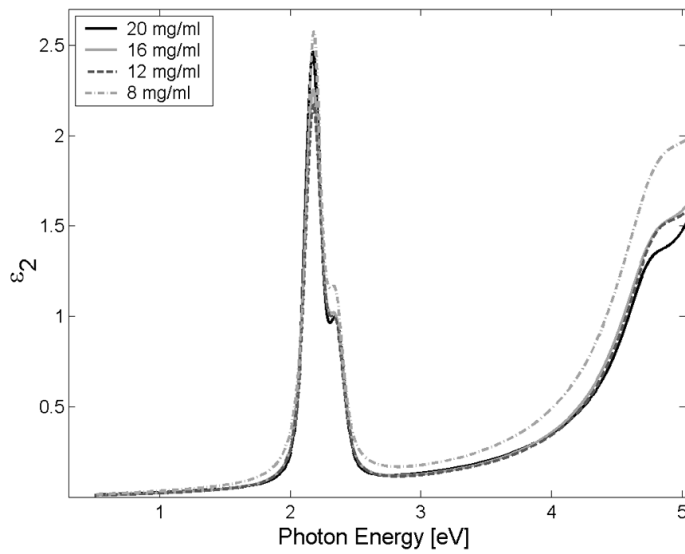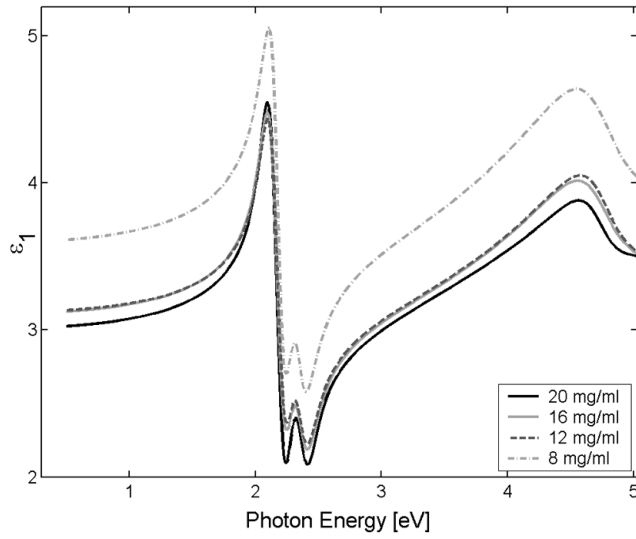
Figure 3a and b. Optical properties extracted from ellipsometric data from samples with RB-films prepared from different solution concentrations.

The double resonances En_1 and En_2 were modeled using a GLAD model, which gave lower parameter correlation. In the GLAD model broadening values Br_1 and Br_2 can not be determined individually and are set equal.

In Fig. 4, representative optical properties of RB from 5.03 eV extended into the IR-region (0.038 eV) are presented. The dielectric function values were extracted from the sample with a RB film made from a solution concentration of 12 mg/ml. The prominent resonances in the wavelength region at 2.18 eV (560 nm) and 2.35 eV (520 nm) and the broader features seen above 4 eV are given in Table 3. The resonance can be compared with the absorption spectra in the literature [3, 18, 19] . The resonance energies are dependent on the solvent. [18, 19] It can be noticed that no dominant absorbance peaks are found in the infrared wavelength region even though several characteristic carbon-oxygen groups usually are seen in this range [20]. The absence of absorption bands from C-H, C-Cl, C-O and C-I bending and stretching vibrations in the 0.1-0.5 eV (12.4 – 2.48 μm, 807 - 4033 cm^{-1}) region of the ellipsometrically determined spectra can be explained by the small sensitivity of the ellipsometric set-up for the low cross section absorption bands in thin films. Since ellipsometry also has a relatively low out-of-plane sensitivity, an orientation effect might also conceal bands if the molecules lie parallel to the surface with the dipole moment of a vibration perpendicular to the surface normal [21].

When studying the switching properties of RB films it is clear that the optical properties of RB before and after exposure to HCl and NH_3 vapor show substantial differences in the visible range. This is presented in Fig.5 and Table. 4 for real time measurements on
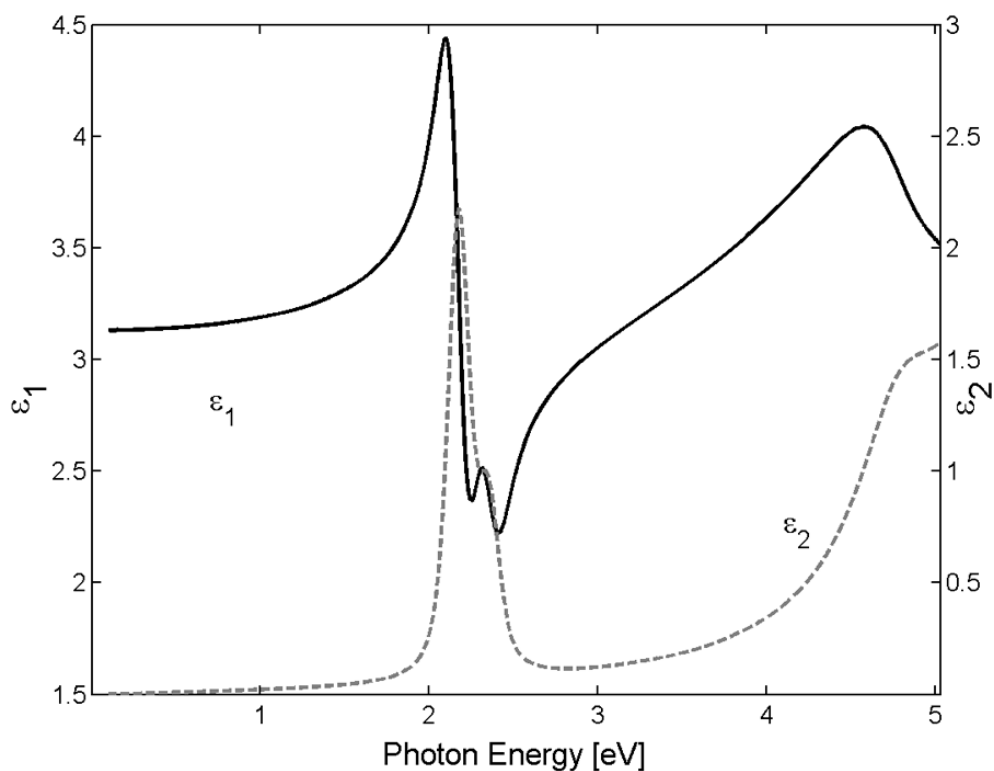
Figure 4. Optical properties of a 20.7 nm layer of RB in terms of the real (—) and imaginary (---) part of the dielectric function in the range 0.038-5.03 eV.

Table 4. Thicknesses of an RB layer prepared from a 12 mg/ml solution in the pristine state (q), after HCl exposure (l) and after NH_3 exposure (q).

Conformational state	Pristine (q)	HCl (l)	NH_3 (q)
Thickness of RB-layers [nm]	21.8	19.8	23.8
Thickness of roughness layer [nm]	2.2	5.2	1.8
Roughness / Total thickness [%]	9.3	20.9	7.1

a film prepared from 12 mg/ml solution. The film is the same as presented above. The switching studies were done, as soon as access to spectroscopic real time measurements was possible, five months after the initial studies on pristine material. After HCl exposure of a pristine quinoid film, the pronounced peaks between 2 and 3 eV were heavily suppressed but the low-energy part of the double resonance is still visible. This
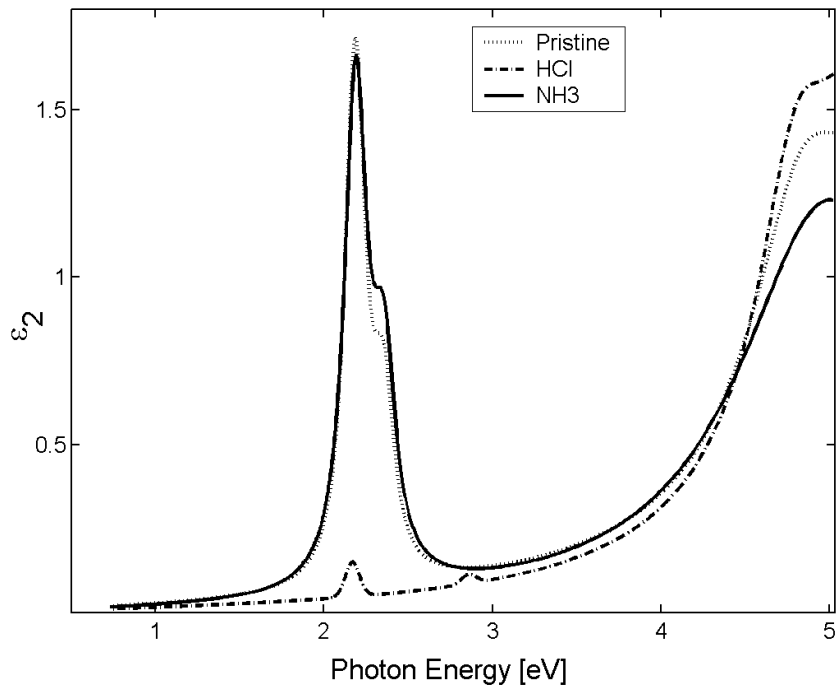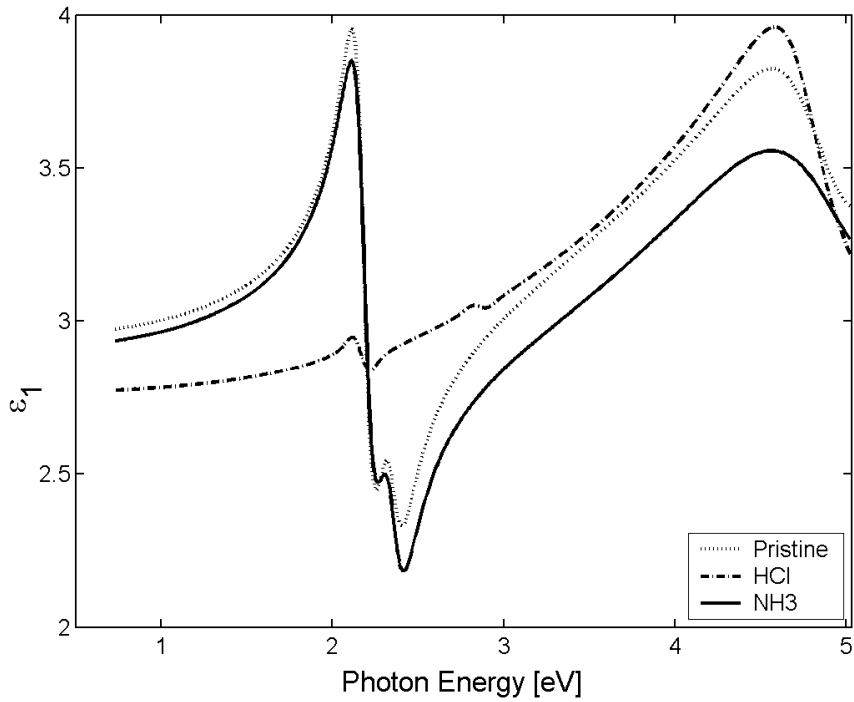
Figure 5a and b. Optical properties of a RB film before and after chemical exposure of HCl and NH₃ with thickness 21.8 nm in the pristine state.

is observed as a color change of the RB film from pink to transparent. In addition, a

small peak appears at 2.9 eV. This indicates that the film is not in a pure l-form but

rather an intermediate state. A subsequent exposure to NH_3 vapor reverses the process making the optical spectra to return close to those for the pristine quinoid state. The peaks above 4 eV are less affected by the HCl/NH_3 exposure.

In the switching studies it was found that the total thicknesses including surface roughness essentially was the same after chemical exposure (Table. 4) except for a small increase in the RB-thickness. Larger thickness changes are not expected since it has been shown [4, 18] that the aromatic ring is perpendicular to the xanthene in both the q- and the l-form of RB. The lactone is connecting the chromophore and xanthene moieties locking the molecule and preventing conformational changes [18]. It is therefore most likely that there will be no rotation of the molecules during switching which could have caused a large change in thickness [22]. In addition to the small thickness increase of the RB-layer there is a decrease in ε_1 which indicates a less dense film after the HCl/NH_3 exposure. The thickness of the modeled roughness layer of the l-form is also found to be larger (Table 4).

Preliminary long time studies showed that the prominent ε_2-peak about 2.18 eV in the pristine quinoid state became less pronounced with time. The time difference between the basic characterization studies and the switching studies is a probable explanation for the difference in optical properties as seen in Fig. 4 and Fig. 5 (pristine). In addition, the switching properties in terms of the effects of exposure to HCl and NH_3 were degraded and the prominent peak did not completely recover after exposure and did after some time decrease even more. Peaks also appeared in the assumed lactone state, which already were observed in the switching studies (see Fig. 5).

The long-time behavior could be explained in terms of transformations between intermediate states due to changes in the surrounding hydrogen bonding environment, which strongly influences the spectral properties [18, 23], and in terms of endeavor for equilibrium between the original specimen and the intermediate that will be formed over time [19]. Another effect that can impair the photochemical response is aggregation [17, 19]. A lower level of the shoulder to the right of the main peak can be caused by this as discussed by Lamberts et al [18].

In conclusion we have used variable angle of incidence spectroscopic ellipsometry to provide optical reference data for thin spin-coated films of a Rose Bengal derivative for photon energies from 0.038 eV to 5.03 eV. In addition typical film thicknesses and surface roughnesses were related to the solution concentration of RB in the spin coating process. For preparation of spin coated RB-films with low roughness it is important to use sufficiently high solution concentration of RB. The optical properties before and after chemically induced switching upon exposure of HCl and NH_3 were also presented.

Acknowledgements

References:

1. P. Andersson, Thesis No. 1237, Department of Science and Technology, Linköping University, Sweden, 2006.

2. P. Chandrasekhar, B. J. Zay, T. McQueeney, A. Scara, D. Ross, G. C. Birur, S. Haapanen, L. Kauder, T. Swanson, D. Douglas, Synth. Met. 135/136 (2003) 23.

3. N. Stevens, PhD Thesis, Chemistry department, The City University of New York, USA, 2006.

4. R. Muthyala, Chemistry and applications of leuco dyes, Topics in applied chemistry, Plenum Press, New York, 1997.

5. B. Pradhan, A. J. Pal, Sol. Energy Mater. Sol. Cells 81 (2004) 469.

6. F. L. E. Jakobsson, X. Crispin, M. Cölle, M. Büchel, D. M. de Leeuw, M. Berggren, Org. Electron. 8 (2007) 559.

7. A. Bandhopadhyay, A. J. Pal, J. Phys. Chemistry B 107 (2003) 2531.

8. S. Karthäuser, B. Lüssem, M. Weides, J. Appl. Phys. 100 (2006) 094504.

9. A. K. Rath, A. J. Pal. Org. Electron. 9 (2008) 495.

10.   J. A. Woollam Co., Inc, WVASE manual, "Guide to using WVASE 32 ^{TM}", 1999, Genosc layer.

11.   F. L. Pedrotti S. J., L. S. Pedrotti, Introduction to optics, Prentice-Hall International Editions, 1993, p.119.

12.   E. Hecht, Optics, Addison-Wesley Publishing Company, 1987.

13.   J. A. Woollam, Ellipsometry, variable angle spectroscopic, in J. G. Webster (ed), Wiley Encyclopedia of Electrical and Electronics Engineering, Supplement 1, , John Wiley and Sons, Inc., 2000, p.111.

14.   C. M. Herzinger, B. Johs, W. A. McGahan, J. A. Woollam, W. Paulson, J. Appl. Phys. 83 (1998) 3323.

15.   D. E. Aspnes, J. B. Theeten, F. Hottier, Phys. Rev. B 20 (1979) 3292.

16.   K. Järrendahl, H. Arwin, Thin Solid Films 313/314 (1998) 114.

17.   C. -C. Chang, Y. -T. Yang, J. -C. Yang, H. -D. Wu, T. Tsai, Dyes Pigm. 79 (2008) 170.

18.   J. M. Lamberts, D. R. S. Joseph, D. C. Neckers, J. Am. Chem. Soc. 106 (1984) 5879.

19.   J. J. M. Lamberts, D. C. Neckers, Tetrahedron 41 (1985) 2183.

20.   A. L. Smith, Applied infrared spectroscopy, Fundamentals, Techniques, and Analytical Problem-Solving, A series of monographs on analytical chemistry and its applications, vol. 54 in Chemical Analysis, John Wiley & Sons Inc., New York, 1979.

21.   A. N. Parikh, D. L. Allara, J. Chem. Phys. 96 (1991) 927.

22.   F. L. E. Jakobsson, PhD Thesis No 1203, Department of Science and Technology, Linköping University, Sweden, 2008.

23.   N. Klonis, W. H. Sawyer, Photochem. Photobiol. 72 (2000) 179.

24.   M. E. Daraio, E. S. Román, Helv. Chim. Acta 84 (2001) 2601.